SAND2012-9120C

Efficient Method of Measuring Effective Mass of a System

Randy L. Mayes
Tyler F. Schoenherr
Jill Blecke
Daniel P. Rohe
Experimental Mechanics, NDE and Model Validation Department
Sandia National Laboratories*
P.O. Box 5800 - MS0557
Albuquerque, NM, 87185
rlmayes@sandia.gov
tfschoe@sandia.gov
jblecke@sandia.gov

Nomenclature

DoF	degree of freedom
FRF	frequency response function
f	force
mm_k	modal mass for mode k
k	spring rate
m_i	mass at DoF i
M_B	mass of the fixture or base
pmpf(k)	pseudo-modal participation factor for mode k
P_k	modal participation factor in one direction for mode k
v	velocity in one direction
x	displacement in one direction
$\ddot{x}$	acceleration in one direction
q	generalized coordinate
$\mathbf{L}$	reduction matrix applying the constraint to equations of motion
Φ	rigid body mode shape vector with ones in the direction of interest
Θ_c	mode shapes of the fixture to be constrained
ζ	modal damping ratio
ω	angular frequency (radians/second)
Ψ	mass normalized real mode shape matrix
Γ	eigenvectors resulting from constraint equations
B	subscript for the fixture or base
c	subscript for degrees of freedom on fixture to be constrained to zero
i	subscript for DoF number
k	subscript for mode number
TA	subscript for the test article

*Sandia is a multiprogram laboratory operated by Sandia Corporation, a Lockheed Martin Company, for the U.S. Department of Energy under Contract DE-AC04-94AL85000.

1) Abstract

Effective mass is a system property that is used in the aerospace industry in predicting the forces of an elastic payload on the delivery system in a specific direction. Effective mass is usually calculated with the finite element model. Experimental effective mass can be used to validate calculated effective mass from a finite element model. Measuring the effective mass of a system, however, has been difficult and has been attempted by putting force sensors between the payload and a test base. A much more tractable method amenable to a payload mounted on a slip table is provided here. The method measures a driving point and a base frequency response function and uses a recently developed method to constrain the base response and calculate the effective mass. This theory will be demonstrated with an analytical system and example hardware.

Keywords – Effective Mass; Modal Participation Factor; Experimental

2) Motivation

Sandia National Laboratories has at least three motivations for having measured effective mass values for the modes of a base mounted payload in a specific direction. The first motivation comes from satellite payload applications. When performing loads analysis to determine the loads a payload puts back into the delivery bus during launch, the modes with high effective mass put high loads back into the bus. Classically, effective mass is calculated from the finite element model, but if the effective mass of the model is wrong, the loads analysis will be wrong. It would be of value to validate the model with test measured effective mass to greatly enhance the confidence in the loads analysis.

The second motivation is associated with the methodology now being utilized at Sandia to quantify margin. This methodology requires a modal model with the modal masses scaled so that the effective mass of each mode in the various shock or vibration test axes are known. Again, this information has always come from a finite element model in the past, but in some cases finite element models have not been generated. It would be of value to extract a modal model experimentally with the associated effective masses for each important mode in the various test axis directions. Then the margin quantification could proceed without the finite element model. Even if the finite element model is available, to check its effective masses against test data would provide a valuable check on the model for the margin calculation.

A third motivation is for vibration control. In certain cases force limiting is practiced to remove over-conservative effects of enveloping test environments. Knowing the effective mass of the test article would allow notching of acceleration inputs without installing force gages under the test article, because the effective mass and input accelerations could be used to limit the force into the structure.

3) Effective Mass Concept and History

The effective mass offers a physical interpretation of a physical system with multiple modes of vibration being excited dynamically from a base, similar to testing that occurs for many systems. The concept was proposed in the early 70's by Bamford[1] with others. For a base excited system, it is represented as attached to a massless base, which will be excited in only one direction with acceleration, $\ddot{x}$, with each mode represented by a single degree of freedom oscillator as shown in Figure 1. The mass of each oscillator is valued so that it is the effective mass of the respective mode of vibration. The springs are scaled so that the mass vibrates at the appropriate modal frequency. In general, only the modes that have the significant effective masses are required to represent the response up to some desired frequency. In the figure we show four such modes. The other modes are truncated. The effective mass of all the truncated modes is added directly to the base as a residual mass. When the base is accelerated with some vibration specification, the various effective mass oscillators will impose the correct reaction force on the base in the direction of excitation. As can be seen from this illustration, effective mass is based on a system that can be represented as having a base input. It depends also on the assumption that the base is rigid.

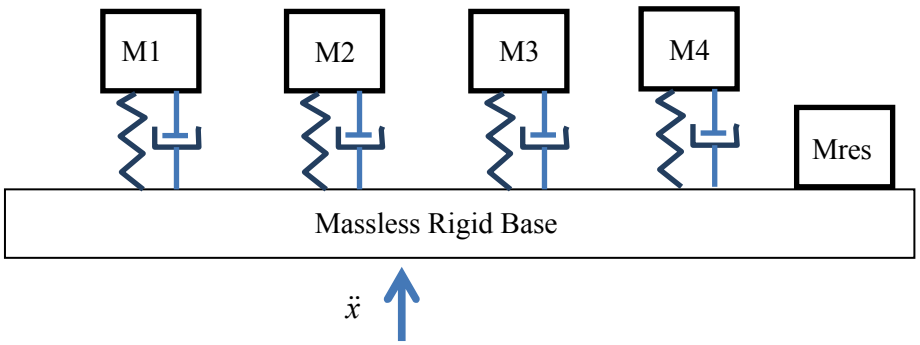

Figure 1 - Physical Picture of Effective Mass Concept

Effective mass is related to modal participation factor, P_k. The derivations of modal participation factor and effective mass can be found in the FEMA 451B Topic 4 Notes [11]. A major difference between effective mass and modal participation factor is that modal participation factor is different depending on the scaling of the modal mass, mm_k, whereas effective mass is a single defined value. In a fixed base eigenvalue problem of an analytical model of the system, the modal participation factor multiplied by $-\ddot{x}$ provides the modal force that will excite a particular mode for the rigid base acceleration, $\ddot{x}$. The effective mass, which provides the actual base reaction force associated with a particular mode, resolves any question about mode shape scaling and is calculated as

$$m_{eff,k} = P_k^2 mm_k . \tag{1}$$

If Ψ_{fixed}^k is the fixed base mode shape vector for mode k and $\mathbf{M}$ is the mass matrix of the test article, the modal participation factor can be calculated from the rigid body mode shape vector, Φ, of the system released and translating in the direction of acceleration of the base as

$$P_k = \overline{\Phi}^T \mathbf{M} \overline{\Psi}_{fixed}^k / mm_k \tag{2}$$

where the rigid body shape values of vector Φ in the direction of acceleration are equal to one and in orthogonal directions are equal to zero. The modal participation factor and effective mass are related to direction. If vector Φ represents the rigid body mode shape in the y direction, as opposed to the x direction as shown in the figure, a different modal participation factor (and effective mass) will be calculated for mode k.

As can be seen, this standard approach requires a finite element model. If the finite element model is in error, the modal participation factor and effective mass will be in error. One method of attempting to extract the modal participation factor and effective mass is to sandwich force gages or a so-called force measurement device between the test article and the shaker table and measure those forces and extract modal parameters from the system during a vibration test[2-4]. Even such a measurement generally assumes the shaker table is rigid. Sedaghati, Soucy and Etienne[5] did this placing eight triaxial force gages beneath a payload during a vibration test. They checked their results by comparing with the effective mass of a finite element model. One of the larger effective mass measurements was within seven percent but two were off by greater than 40 percent and the effective mass of the first mode was off by hundreds of percent. They claimed the error was due to nonlinearity, but the FRF showing the apparent mass appeared to retain the shape one would expect for the first mode of a linear system. This also required an in situ re-calibration of the force sensors to match the measured mass of the test article, which demonstrates the difficulty of trying to obtain force measurements in a sandwich configuration.

4) Effective Mass Measurement Approach

Here the authors propose an approach logistically simpler than measuring all the forces of attachment of a structure to a slip table. It may be applied to any fixture which has at least one rigid body mode (a mode low enough in frequency that it can be considered to be represented purely by rigid body motion), as well as to a shaker table (which always has a rigid body mode in the direction it is designed to shake). The method does not require a rigid base assumption as with the sandwiched force measurement device. The natural dynamics of the shaker table or fixture are measured and then analytically constrained to provide a mathematical rigid base. The method builds on previous work which has been used to calculate fixed base mode shapes from experimental modal parameters extracted from a test article mounted to a shaker table or other dynamic fixture. Mayes and Bridgers[6] first showed that one could perform a modal analysis of a test article on a plate and analytically fix the modes of the plate so that the resulting constrained modes approximated the fixed base modes. Since then several

refinements and studies have been performed[7-9]. This capability to analytically constrain the system inherently contains enough information to calculate the effective mass in directions well excited by the modal test, if one knows the mass properties of the fixture to which the test article is attached. From this point forward, the "fixture" refers to the base to which a test article is attached, whether it is a shaker table or some other system.

This approach will be demonstrated with a simple MATLAB spring mass model and an experimental system. The experimental system is shown set up on a slip table in Figure 2. The test article is a nylon beam-like structure.

Figure 2 - Experimental Test Article Mounted on Slip Table

5) Effective Mass Measurement Theory

Begin with a system that has one rigid body mode in the direction of the desired effective mass estimate. Let us consider an example multi-degree of freedom system as shown in Figure 3.

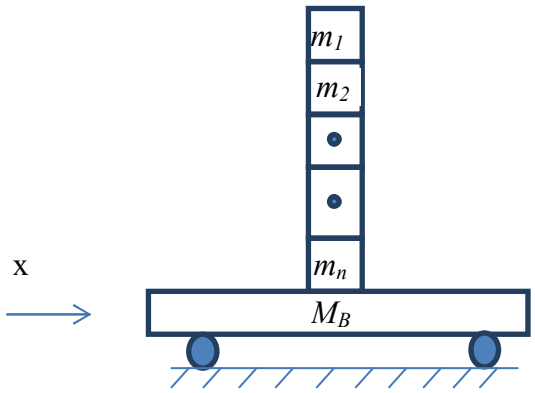

Figure 3 - Simple Analytical Base Mounted Test Article

The system has one rigid body mode in the x direction of motion. The mass of the base, M_B, is known. The multi-degree of freedom test article is represented by masses m_1 through m_n. Although the individual masses are not known, the test article total mass, which is the sum of m_1 through m_n, is known. The base cannot rotate, and is considered a rigid mass that may only move in the x direction. One performs a modal test on this system and at least determines the modal parameters and the mode shape of the base for the rigid body mode and several elastic modes, which we will call Ψ_B.

Recalling eqn (2) as

$$P_k = \overline{\Phi}^T \mathbf{M} \overline{\Psi}^k_{fixed} / mm_k \tag{2}$$

the first question is how can we get Ψ^k_{fixed} ? In the appendix, the equations to constrain the experimental mode shapes obtained from the test of Figure 3 are given providing

$$\Psi_{fixed} = \Psi \mathbf{L} \Gamma \tag{3}$$

so that Ψ^k_{fixed} can be determined from

$$\Psi^k_{fixed} = \Psi \overline{\mathbf{a}}_k \tag{4}$$

where the vector $\overline{\mathbf{a}}_k$ is the kth column of $\mathbf{L}\Gamma$. Assume the mode shapes are scaled for unit modal mass and substitute eqn (4) into eqn (2) to give

$$P_k = \overline{\Phi}^T \mathbf{M} \Psi \overline{\mathbf{a}}_k \tag{5}$$

Which can be expanded as

$$P_k = \left[\overline{\Phi}^T \mathbf{M} \overline{\Psi}_1 \quad \overline{\Phi}^T \mathbf{M} \overline{\Psi}_2 \quad \ldots \quad \overline{\Phi}^T \mathbf{M} \overline{\Psi}_n \right] \overline{\mathbf{a}}_k \quad . \tag{6}$$

Let us define each term in the brackets in eqn (6) as a pseudo-modal participation factor (*pmpf*). It is prefixed with "pseudo" because we obtain it with the base mass free to move, instead of fixed, as in the strict definition of modal participation factor. Each of the pseudo-modal participation factors considers the mode shape of the entire test article, but NOT the base. One must determine each of these *pmpf* s. For the first mode, which is the rigid body mode translating in x, we can note that

$$\overline{\Phi}^T \mathbf{M} = \left[m_1 \quad m_2 \quad \ldots \quad m_n \right]_{TA} \tag{7}$$

Which gives a row vector of all the masses of the test article, subscript TA, and

$$\overline{\Psi}_1 = \begin{Bmatrix} 1 \\ 1 \\ \dots \\ 1 \end{Bmatrix} \Psi_B^1 \quad . \tag{8}$$

Combining eqn(7) and (8) yields the first pmpf from the rigid body mode as

$$pmpf(1) = \overline{\Phi}^T \mathbf{M} \overline{\Psi}^1 = \begin{bmatrix} m_1 & m_2 & \dots & m_n \end{bmatrix}_{TA} \begin{Bmatrix} 1 \\ 1 \\ \dots \\ 1 \end{Bmatrix} \Psi_B^1 = m_{TA} \Psi_B^1 \quad . \tag{9}$$

This requires only two values, the known mass of the test article without base, m_{TA} , and Ψ_B^1 which is the measured base rigid body mode shape (mass normalized) in the desired direction. Though the individual elements of the mass matrix are not known in a hardware modal test, both terms are known on the right hand side if one extracts the mode shape of the base and weighs the test article.

The *pmpf* for any other elastic mode may be obtained from conservation of momentum. Assume we excite only one of the elastic modes, *k*, in an undamped sense. Then the momentum sum is

$$\sum_{i=1}^{n} m_i v_i + M_B v_B = 0 \tag{10}$$

where *v* is the velocity . The velocity can be replaced with the modal substitution to give

$$(\sum_{i=1}^{n} m_i \Psi_i^k + M_B \Psi_B^k) \dot{q} = 0 \tag{11}$$

with *q* as a generalized coordinate. Dividing by the generalized velocity and noting that the summation term is equal to the *pmpf*(k) gives

$$pmpf(k) = \Phi^T \mathbf{M} \Psi^k = \sum_{i=1}^{n} m_i \Psi_i^k = -M_B \Psi_B^k \quad . \tag{12}$$

The *pmpf* for each elastic mode comes simply from the mass of the base and the mode shape of the base. Now all quantities are know so eqn (9) and (12) are substituted into eqn (6) to give the estimate of the true modal participation factor, P_k, from which effective mass can be obtained in eqn (1). In review, $\overline{\mathbf{a}}_k$ is the *k*th column of $\mathbf{L}\Gamma$, pmpf(1) comes from the mass of the test article and the rigid body mode shape of the base, and the elastic *pmpf*(*k*) are determined from the mass of the base and the test mode shape of the base. The resulting modal participation factor, P_k, is subject to errors of modal truncation.

The previous derivation shows how to estimate the effective mass from modal parameters for the described system which has only one unconstrained DoF for the base motion. However, most systems are not constrained with only one base DoF as the described system. They may have more than one rigid body mode of the fixture, and there may be other elastic modes of the fixture. Here we follow the previous work[6-9]. One performs a modal test on the system and fixture with enough accelerometers mounted on the fixture to uniquely identify every different shape active in the fixture. These fixture shapes are then captured as multiple independent vectors in Θ_c. One of those vectors, noted as vector *j*, should be rigid body motion that is purely in the x direction of Figure 3. Eqn (A4) provides the required constraint, except that row j should be removed from the constraint. This allows the system to have rigid body motion in the one desired direction as depicted in Figure 3, while constraining all other rigid body and elastic motions. The appendix equations with the required adjustment to eqn (A4) recasts the original dynamics to those of a problem constrained as defined in Figure 3.

To review, one performs a forced modal test on the system. Enough accelerometers on the fixture must be placed so that the active rigid and elastic shapes may be captured with independent fixture shapes, Θ_c. The appendix equations are applied to obtain a system that is constrained similar to that shown in Figure 3. Then use the partially constrained modal parameters, the mass of the base and the mass of the test article to calculate the pseudo-modal participation factors. Finally constrain the final rigid body DoF and determine the modal participation factors and resulting effective masses from eqn (1) and (6).

6) Analytical Example

Consider a spring mass system with three DoF as shown in
Figure 4. Here, M_B is the mass of the base and m_1 and m_2 are associated with the masses of the test article. So the total mass of the test article is $m_{TA}= m_1+ m_2$. For this configuration, the system has one rigid body mode. One might imagine M_B as the slip table and m_1 and m_2 as the test article mounted to the slip table.

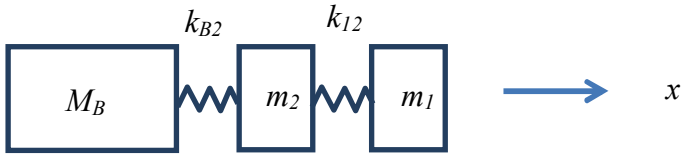

Figure 4 - Analytical Example 3 DoF System

One desires to perform a modal test of this system, with accelerometers mounted on the base. The mass of the base, M_B , and the mass of the test article, m_{TA}, are known. From the modal test three modes are extracted with mass normalized mode shapes of the base. The first mode is a rigid body mode. Then one desires to analytically fix the base, and get the modal participation factors of the test article and the effective mass for the two remaining modes in the x direction. The parameters used in this example are M_B= 500, m_1= 2, m_2= 5, m_{TA} =7 , k_{B2}= 10,000, k_{12}= 10,000. Using eqns(4,7,8-19) the effective mass for the first and second modes of the fixed base system are computed as 6.8577 and 0.1423, which match the true values calculated for a fixed base system from eqn (1,2). Also, the sum of all the effective masses in one direction are equal to m_{TA} , which is seven for this case.

7) Hardware Example on Small Seismic Mass

The first hardware test setup is shown in Figure 5. The test article is a 72 kg nylon beam and the fixture is a 605 kg steel seismic mass which was instrumented with four triaxes at the corners. The test article and seismic mass were suspended with straps, yielding rigid body modes below five Hz. A modal test was performed using a random shaker input and modes were extracted using SMAC[10]. Three input locations near the top of the beam were excited. Effective mass was extracted for the first ten modes to 1350 Hz in the softer bending direction of the beam. The seismic mass had one elastic classic plate mode at 1370 Hz, and it was constrained along with the rigid body modes of the mass for this analysis. One of the x direction accelerometers on the mass was found to have low amplitude, so it was excluded from the analysis. The beam was modeled with finite elements (FE) in SALINAS and the uncertain Young's modulus and Poisson's ratio were adjusted to best match the test data. All the first ten modes in the soft bending direction matched within two percent between the test and FE model. The effective masses are compared in Table 1, expressed as a fraction of the total test article mass. The difference column is the difference expressed as a percentage of the total test article mass. Most of the agreement is within two percent of the total test article mass. Interestingly, the very first mode is the worst comparison, with the values about eight percent different, which is an error that is a little over three percent of the total mass.

Table 1- Test Effective Mass from Seismic Mass Test Compared to FE Model

Test Frequency (Hz)	Effective Mass from Test	Effective Mass from FE Model	Difference as % of Total Test Article Mass
38.94	0.415	0.448	3.3
163.5	0.187	0.189	0.2
396.3	0.088	0.085	-0.4
706.4	0.037	0.047	1.0
859.2	0.004	0.000	-0.4
1034.7	0.011	0.000	-1.1
1048	0.003	0.023	2.0
1190.7	0.000	0.000	0.0
1316.1	0.027	0.004	-2.3
1344.3	0.020	0.004	-1.6

It was noted above that one of the accelerometers on the base that measured motion in the direction of the desired effective mass was excluded from the analysis. It appeared to be reading about 20 percent lower than the others for modes with fairly pure motion in that axis. When that accelerometer was included in the analysis, the difference from the FE calculation in the first test effective mass more than doubled. This result underscores the need for very accurate absolute measurements on the fixture structure.

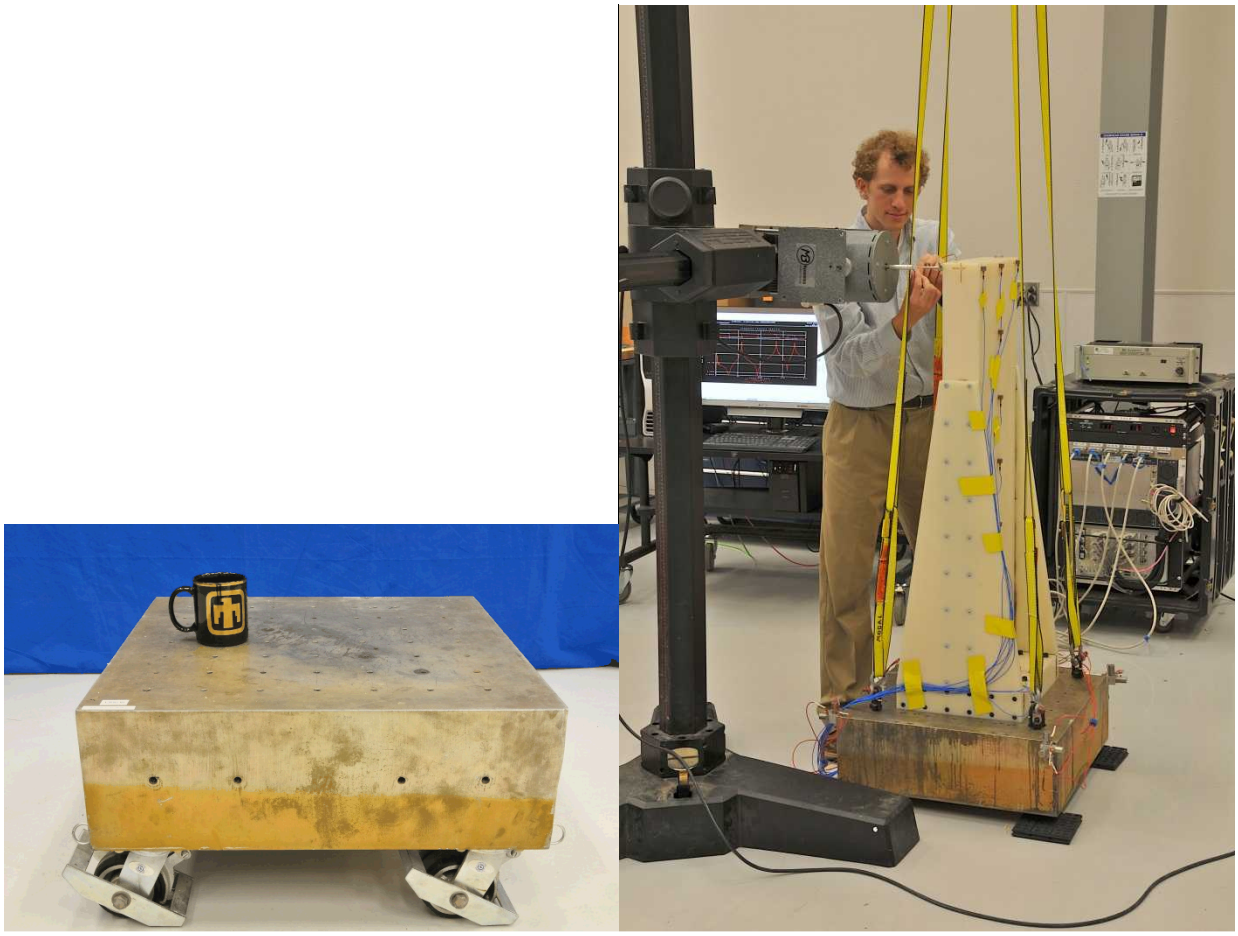

Figure 5 - Small Seismic Mass (left) and Test Article Setup (Right)

8) Hardware Example on Slip Table

The same test hardware was used on a slip table with the same theory. In this case only two fixture modes were present. One was a rigid body mode of the slip table at 0 Hz and one was the first extensional mode of the slip table at 2035 Hz. In this work, a portable shaker was attached to the slip table with a force gage and the slip table was not connected to the large shaker that normally drives it. The test setup is shown in Figure 6. Seven triaxial accelerometers were mounted on the slip table and used for the constraint analysis. The modal test utilized random input, and the modal extraction was performed with SMAC. Very similar test effective mass results were obtained from this separate setup and are given in Table 2.

Table 2 - Effective Mass Extracted from Slip Table Test Compared to FE Model

Test Frequency (Hz)	Effective Mass from Test	Effective Mass from FE Model	Difference as % of Total Test Article Mass
38.2	0.413	0.448	3.5
162.3	0.177	0.189	1.2
393	0.080	0.085	0.5
701.5	0.051	0.047	-0.4
852.9	0.000	0.000	0.0
1028	0.033	0.000	-3.3
1040	0.018	0.023	0.5
1199	0.000	0.000	0.0
1301	0.001	0.004	0.3
1344	0.001	0.004	0.3

Figure 6 - Test Article Mounted on Slip Table with Portable Shaker

9) Conclusions

This paper develops the theory to calculate effective mass from a standard modal test of a test article on a fixture, when the fixture has at least one rigid body mode in the direction of the desired effective mass calculation. The strength of the theory is verified by an analytical example. It is then applied to two different test setups for the same test article. In one setup, the

test article is mounted on a seismic mass and suspended softly with straps. In the other setup, the test article is mounted on a slip table for a shaker. The effective mass for each mode in one direction is extracted from the tests and compared to a FE model effective mass calculation for the test article. (The FE model Young's modulus and Poisson's ratio were calibrated so that the frequencies of the FE model match the test within two percent). The test effective mass calculations agree with the FE calculations within about four percent of the total mass of the test article. The first mode has the greatest test effective mass, and is the most different from the FE model calculation. Agreement for the test effective mass between the two tests is very consistent, being within about one percent of the total mass, even though the setups were quite different. It is not known whether the difference between the test effective mass and the FE effective mass in the first mode is due to test error or FE error.

10) Appendix – Constraining a system with one rigid body mode to fixed base

The system of Figure 3 can be modeled, neglecting damping, as

$$\left[\omega_{n}^{2}\right]\{q\}-\omega^{2}[I]\{q\}=\Psi^{T}\{f\} \tag{A1}$$

where ω_n represents the circular natural frequencies, q represents the modal coordinates, f is the vector of forces. A constraint for the fixture (subscript c) DoF can be written as

$$\{x_c\}=\{0\} \tag{A2}$$

or using the modal substitution, then

$$\Psi_c\{q\}=\{0\}. \tag{A3}$$

Generally, with the authors' method, there will be many accelerometers mounted on the fixture represented by the lower mass, M_B. One may convert from many physical DoF constraints of eqns (A2) and (A3) to one modal constraint with

$$\overline{\Theta}_c^{+}\Psi_c\{q\}=\{0\} \tag{A4}$$

Where the vector Θ_c comes from an estimate of the single translation rigid body mode shape vector of the fixture. The superscript + indicates the pseudo-inverse. This projects the constraint onto the vector space of Θ_c, which has the advantage of producing a least squares fit through any experimental modal analysis shape errors, since Θ_c has more sensors (rows) than modes (columns). The unconstrained coordinates can be written in terms of a reduced number of unconstrained generalized coordinates as

$$\{q\}=\mathbf{L}\{q_L\}. \tag{A5}$$

Substituting eqn (A5) into eqn (A4) yields

$$\Theta_c^{+}\Psi_c\mathbf{L}\{q_L\}=\{0\}, \tag{A6}$$

where **L** is found as the matrix of vectors that are orthogonal to $[\Theta_c^{+}\Psi_c]^T$

$$\mathbf{L}=null(\Theta_c^{+}\Psi_c) \tag{A7}$$

which satisfies the constraint. Substituting eqn (A5) into eqn(A1) and pre-multiplying by $\mathbf{L}^T$, gives the coupled eigenvalue problem

$$\mathbf{L}^T\left[\omega_{n}^{2}\right]\mathbf{L}\{q_L\}-\omega^{2}\mathbf{L}^T[I]\mathbf{L}\{q_L\}=\{0\}. \tag{A8}$$

If we solve this eigenvalue problem and call the resulting generalized uncoupled coordinates p and the associated eigenvectors Γ, then from the modal substitution and eqns (A2, A3 and A5)

$$x=\Psi\mathbf{L}\Gamma\{p\}. \tag{A9}$$

So the fixed base mode shapes are estimated as

$$\Psi_{fixed}=\Psi\mathbf{L}\Gamma. \tag{A10}$$

Eqn (A10) shows that the fixed base mode shapes are just a linear combination of the original mode shapes associated with the boundary condition of Figure 3.

References

1 Wada, Ben K., Bamford, Robert, and Garba, John A., "Equivalent Spring-Mass System: A Physical Interpretation", *The Shock and Vibration Bulletin*, US Naval Station – Key West, FL, January 1972, pp 215-224.

2 Fullekrug, Ulrich, "Determination of Effective Masses and Modal Masses from Base-Driven Tests", *Proceedings of the 14th International Modal Analysis Conference*, Dearborn, Michigan, February 1996, pp. 671-681.

3 Sinapius, J.M.,, "Identification of Free and Fixed Interface Normal Modes by Base Excitation", *Proceedings of the 14th International Modal Analysis Conference*, Orlando, FL, February 2009, pp. 23-31.

4 Schedlinski, C., and Link, M., "Identification of Frequency Response Functions and Modal Data from Base Excitation Tests Using Measured Interface Forces", *Proceedings of the ASME Conference on Noise and Vibration*, Boston, MA, 1995, ISBN 0-7918-1718-0.

5 Sedaghati, R.,Soucy, Y, and Etienne, N., "Experimental Estimation of Effective Mass for Structural Dynamic and Vibration Applications", *Proceedings of the 21st International Modal Analysis Conference*, Kissimmee, FL, 2003, Paper 188.

6 Mayes, Randy L. and Bridgers, L. Daniel, "Extracting Fixed Base Modal Models from Vibration Tests on Flexible Tables", *Proceedings of the 27th International Modal Analysis Conference*, Orlando, FL, February 2009, paper 67.

7 Allen, Matthew S., Gindlin, Harrison M. and Mayes, Randall L., "Experimental Modal Substructuring to Extract Fixed-Base Modes from a Substructure Attached to a Flexible Fixture", *Proceedings of the 28th International Modal Analysis Conference*, Jacksonville, FL, February 2010, paper 164.

8 Mayes, Randy L. and Allen, Matthew S., "Converting a Driven Base Vibration Test to a Fixed Base Modal Analysis", *Proceedings of the 29th International Modal Analysis Conference*, Jacksonville, Florida, 2011, paper 36.

9 Mayes, Randy L., "Refinements on Estimating Fixed Base Modes on a Slip Table", *Proceedings of the 30th International Modal Analysis Conference*, paper 162, February 2012.

10 Hensley, Daniel P., and Mayes, Randall L., "Extending SMAC to Multiple References", *Proceedings of the 24th International Modal Analysis Conference,* pp.220-230, February 2006.

11 http:/www.ce.memphis.edu/7119/fema_notes.htm, Topic 4 Notes.